FEBS Letters 586 (2012) 526–535

journal homepage: www.FEBSLetters.org

Review

Interfacial electrochemical electron transfer in biology – Towards the level of the single molecule

Jingdong Zhang, Qijin Chi, Allan G. Hansen, Palle S. Jensen, Princia Salvatore, Jens Ulstrup *

Department of Chemistry, DTU Chemistry, Building 207, Kemitorvet, Technical University of Denmark, DK 2800 Kongens Lyngby, Denmark

ARTICLE INFO

Article history:
Received 8 August 2011
Revised 4 October 2011
Accepted 11 October 2011
Available online 20 October 2011

Edited by Miguel Teixeira and Ricardo O. Louro

Keywords:
Protein film voltammetry
Scanning tunneling microscopy
Single-crystal electrode surfaces
Metalloproteins

ABSTRACT

Physical electrochemistry has undergone a remarkable evolution over the last few decades, integrating advanced techniques and theory from solid state and surface physics. Single-crystal electrode surfaces have been a core notion, opening for scanning tunnelling microscopy directly in aqueous electrolyte (in situ STM). Interfacial electrochemistry of metalloproteins is presently going through a similar transition. Electrochemical surfaces with thiol-based promoter molecular monolayers (SAMs) as biomolecular electrochemical environments and the biomolecules themselves have been mapped with unprecedented resolution, opening a new area of single-molecule bioelectrochemistry. We consider first in situ STM of small redox molecules, followed by in situ STM of thiol-based SAMs as molecular views of bioelectrochemical environments. We then address electron transfer metalloproteins, and multi-centre metalloenzymes including applied single-biomolecular perspectives based on metalloprotein/metallic nanoparticle hybrids.

1. Introduction

Interfacial electrochemistry of biological molecules and macromolecules such as redox metalloproteins, their amino acid building blocks, DNA components, biomimetic lipid membranes, and bioinorganic "hybrids" of metallic nanoparticles and metalloproteins, is moving towards new levels of understanding. Key notions are imaging of the biomolecules at the electrochemical interface, and electron transfer (ET) and even enzyme processes followed towards the single molecule level of resolution.

Interfacial electrochemical ET in biology towards unprecedented levels of resolution follows fruitful interactions among several areas, rooted in physical electrochemistry closely associated with surface and condensed matter physics, biotechnology, and new instrumentation. The latter includes scanning tunnelling and atomic force microscopy, operating directly in aqueous biological media under electrochemical potential control (in situ STM and AFM) [1–3]. In situ STM/AFM now extend well beyond imaging (which remains a daunting challenge for large and fragile biomolecules) and has also been brought to map and control biomolecular function such as ET of even large, multi-centre metalloproteins, or protein unfolding and DNA unzipping. The introduction of single-crystal, ("well-defined") atomically planar electrode surfaces was a major breakthrough that also laid the foundation for other electrochemical technology such as a range of spectroscopic surface techniques as well as statistical mechanical and electronic structural theories [4–7]. In addition, in situ imaging of single biomolecules rests on biotechnology such as mutant and synthetic metalloproteins. Altogether this has led bioelectrochemistry towards similar boundary-traversing results as previously in physical electrochemistry.

An essential pre-requisite in protein monolayer voltammetry (PMV) and single-biomolecular ET is understanding of the underlying molecular ET (and proton transfer) processes. Molecular charge transport theory has continued to develop [8–13], more recently as a theoretical frame for in situ STM and other condensed matter single-molecule conductivity phenomena [14]. Single-molecule (in situ) STM mapping rests on molecular tunnelling conductivity, rather than topographic shape. At least two-fold theoretical support is therefore needed. Electronic structure computations have, first disclosed sometimes unexpected, details in the STM contrasts of "small" (bio)molecules such as single amino acids and related molecules [15,16]. Solvation is, further crucial and computationally demanding for in situ STM of electrostatically charged molecules such as functionalized alkanethiol SAMs [17]. Secondly, other new challenges arise for large redox molecules and biological (macro)molecules such as metalloproteins where molecular ET theory has been a powerful tool [14]. By their analytical form, these "phenomenological" theories have offered immediate insight into current/overpotential and other in situ tunnelling correlations and disclosed even new ET phenomena. The combination of protein biotechnology with well-defined (single-crystal) electrochemical interfaces and in situ STM/AFM offer other perspectives

* Corresponding author.
E-mail address: ju@kemi.dtu.dk (J. Ulstrup).

0014-5793
doi:10.1016/j.febslet.2011.10.023

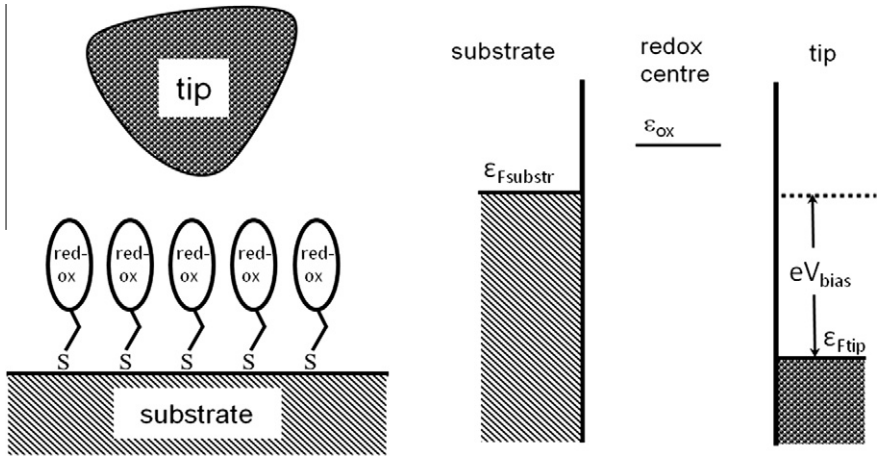

Fig. 1. Left: Schematic view of redox molecules enclosed between a STM working electrode and tip or between a pair of nanogap electrodes. Right: Electronic energy scheme for the redox molecule initially in the oxidized state.

in bioelectrochemical signal transfer between target molecules and external biosensing electrochemical circuitry.

2. Interfacial ET in molecular and protein monolayer voltammetry (PMV)

In situ STM maging and image interpretation rest fundamentally on interfacial electrochemical ET processes. PMV is crucial to control conditions for optimal immobilized protein function. Condensed matter molecular charge transfer theory [8–10,12,13,18] offers comprehensive conceptual support for both bioelectrochemistry of redox proteins, and for in situ STM of complex molecules. The theory addresses, overarchingly: (a) electron tunnelling between the electrode and donor or acceptor groups in the biomolecules through intermediate protein "matter", and (b) the nuclear environmental effects from local, collective protein or DNA, and solvent nuclear modes. In situ STM [10,18,19] offers new theoretical challenges.

2.1. Theoretical notions of interfacial chemical and bioelectrochemical ET

Views of the electrochemical ET process carry over to (bio)electrochemical nanoscale systems. Notions in focus are illuminated by the following cathodic current density form (with an analogous anodic form) broadly valid but with recognized limitations [8,9]:

$$j(\varepsilon;\eta) = e\Gamma_{ox}^{\frac{1}{2}}\Gamma_{red}^{\frac{1}{2}}\kappa_{eff}\frac{\omega_{eff}}{2\pi}\exp\left[-\frac{(E_R+e\eta)^2}{4E_Rk_BT}\right] \quad (1)$$

Γ_{ox} and Γ_{red} are the populations of the oxidized and reduced state of the (bio)molecule at the electrode surface, e the electronic charge, E_R the nuclear reorganization free energy, η the overpotential, ω_{eff} the effective nuclear vibrational frequency of all the nuclear modes reorganized, k_B Boltzmann's constant and T the temperature. κ_{eff} is the electronic transmission coefficient the most important part of which is the electron exchange energy, which couples the molecular acceptor level (A) with metallic electronic levels around the Fermi energy ε_F. Eq. (1) holds an electronic tunnelling factor, κ_{eff}, and a nuclear activation factor that includes contributions from all the protein conformational, and external solvent polarization modes, and the driving force ($e\eta$). Molecular charge transfer theory has developed into much more powerful frames than implied by this simple formalism. A number of these are important in interfacial ET processes of biological macromolecules and covered in a comprehensive literature, overviewed e.g. in [8–10,12,13,18,20,21].

2.2. The reorganization free energy and the electronic tunnelling factor

The reorganization free energy, E_R holds an intramolecular and an environmental contribution. Modified forms of the quadratic

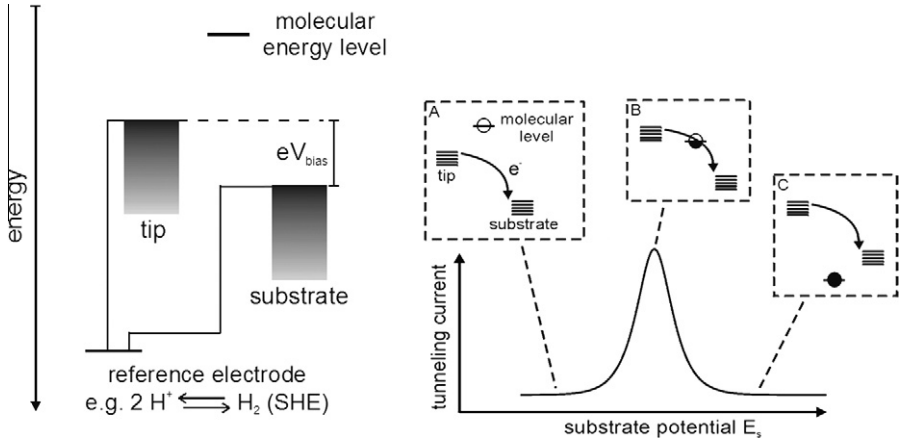

Fig. 2. Left: Electrochemical control of the energy scheme in Fig. 1. The continuous electronic energy spectra of the enclosing electrodes are indicated. The Fermi levels are shifted by the bias voltage energy. Right: Current/overpotential relation on parallel variation of the substrate and tip electrode potentials.

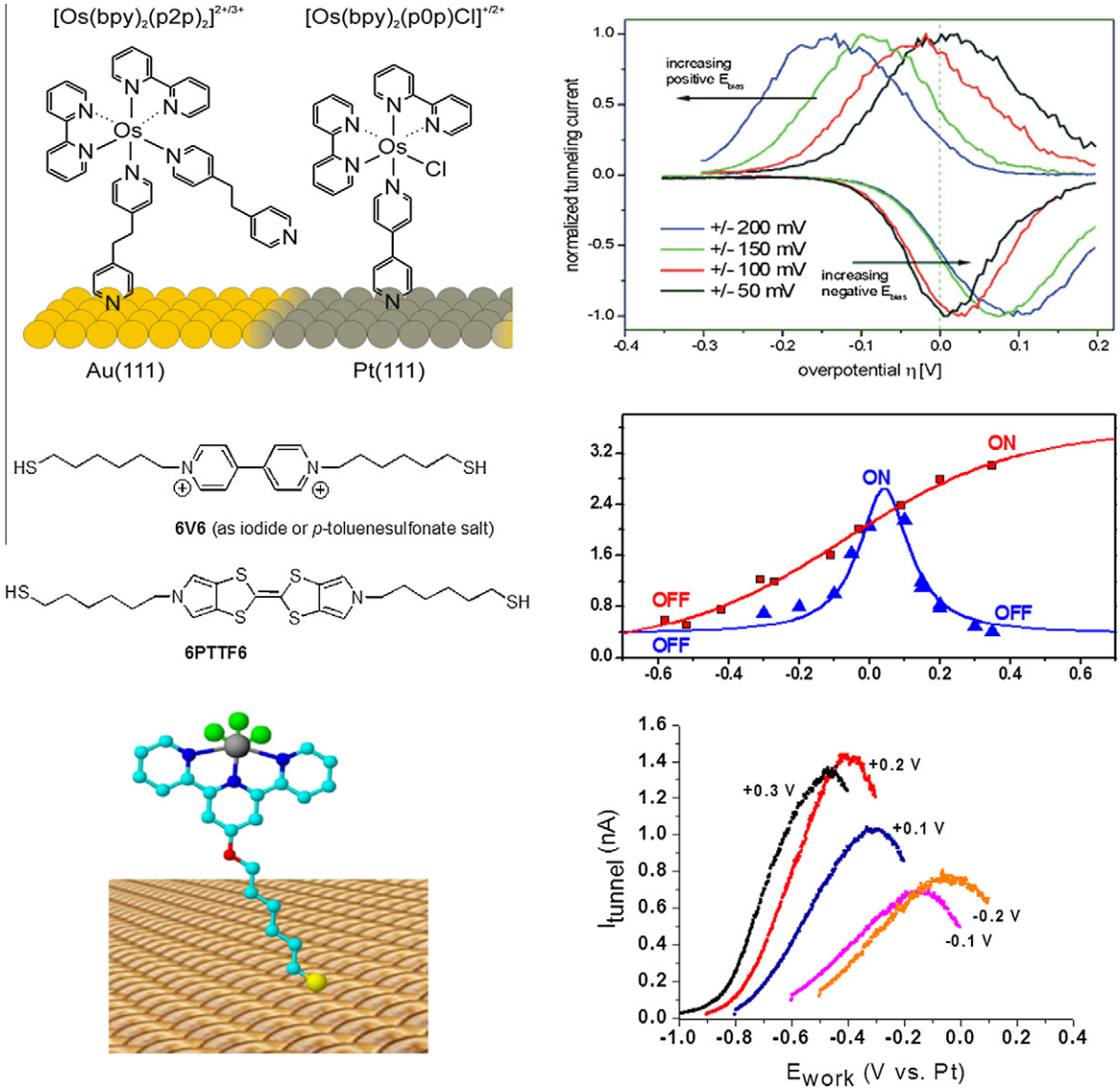

Fig. 3. Three examples of in situ STM and single-molecule in situ STS of small redox molecules. Molecular structures shown in the left column, in situ STS in the right column. Top: two Os-bipyridine complexes on a single-crystal Pt(111)-electrode surface, and in situ tunnelling current/overpotential STS at different bias voltages [27]. Middle: Hexanethiol 4,4′-substituted viologen, 6V6 and 6-*p*-tetrathiafulvalene, 6PTTF6. These two molecules display different tunnelling current/overpotential correlations. This was assigned to a soft molecular structure for 6V6 leading to "gated" tunnelling. No gating is needed for the rigid 6PTTF6 structure [26]. Bottom: In situ metal (Ru(II)/(III)) coordination to immobilized thiol-linked terpyridine ligand. In situ STS at negative bias voltage has been reversed in the diagram [29].

form [8,9,21], Eq. (1) are needed when vibrational frequency changes, nuclear mode anharmonicity etc. are important. This applies e.g. when major local nuclear reorganization accompanies the ET process such as for dissociative ET [22,23] in the blue oxidase Type 3 centres. Nuclear tunnelling is crucial in proton and hydrogen atom transfer processes reflected in sometimes spectacular kinetic deuterium isotope effect. The quadratic activation free energy form, however, rests on the very general assumption that whatever structural features characterize the environment, conformational changes, polarization etc. responds linearly to the electric or other field changes.

Simple analytical forms illustrate the tunnelling "percolation" process through a network of intermediate groups between the electrode and the molecular redox centre(s) in the protein. The electronic transmission coefficient can be given the simple form

$$\kappa_{\mathrm{eff}} \approx \kappa^{0}_{\mathrm{eff}} \exp(-\beta R), \quad \beta \approx \frac{2}{a} \ln \frac{\Delta(\eta)}{\varsigma} R \tag{2}$$

which reflects the directional tunnelling dependence on the ET distance R. The quantity β (length^{-1}) incorporates all information about LUMO or HOMO energetics and local electronic couplings of intermediate amino acid residues, water molecules, linker groups etc. Eq. (2) is coarse-grained over the details of the electron or hole transfer routes [8,9]. The bridge to molecular protein/water/linker properties can be appreciated by the correlation, Eq. (2), right where $\Delta(\eta)$ is the average (electrochemical potential dependent) energy gap between the intermediate group LUMOs or HOMOs and the donor redox level (the Fermi energy of the electrode). ζ is the average electronic coupling between the intermediate groups, and a the average structural extension of each group. Eq. (2) represents directional exponential tunnelling distance decay, with faster decay the larger the energy gap and the weaker the coupling. β in different media accords with

$$\beta_{\mathrm{vacuum}}(\approx 2\text{–}4\ \text{Å}^{-1}) > \beta_{\mathrm{water}}(\approx 1.7\ \text{Å}^{-1}) > \beta_{\mathrm{protein}} (\approx 1\text{–}1.6\ \text{Å}^{-1}) > \beta_{\mathrm{covalent}}(\approx 1\ \text{Å}^{-1}) \tag{3}$$

indicating that protein is a more facile tunnelling medium than water, in turn more facile than vacuum. $\beta_{protein}$ also spans a range of values, with $\beta_{protein}^{\alpha\text{-helix}} > \beta\text{-protein}^{\beta-sheet}$. Eq. (2) applies, further only when the tunnelling barrier is significant, $\Delta(\eta)/\zeta \gg 1$. At small $\Delta(\eta)/\zeta$, tunnelling is replaced by "hopping" through intermediate levels now populated physically with temporarily trapped electrons or holes. This opens a range of ET channels including vibrationally fully or partially relaxed ("dynamically populated") intermediate states [8,9]. The four-heme cyt c_3 class [24] is a possible example for which this notion may hold clues to ultra-fast ET between the closely spaced heme groups.

3. Theoretical notions in bioelectrochemistry towards the single-molecule level

3.1. Some theoretical concepts

We address specifically in situ STM of redox (bio)molecules but concepts and formalism carry over to other metallic nanogap configurations. In addition to the substrate and tip, a third electrode serves as reference electrode. The three-electrode configuration is the basis for *two* kinds of tunnelling "spectroscopy" unique to in situ STM [14]. One is the current–bias voltage relation as in STM in air or vacuum, but with the substrate (over)potential kept constant. The other one is the current-overpotential relation at constant bias voltage, i.e. the substrate and tip potentials are varied in parallel relative to the reference electrode.

Fig. 1 shows a schematic view of a redox molecule in a molecular scale gap between *two* electrochemical metallic electrodes. The Fermi levels of the two electrode surfaces are separated by the bias voltage, eV_{bias}, at given overpotential η. The molecular redox level, say the oxidized, electronically "empty" level is first located above the Fermi energy of the working electrode. Fig. 1 shows explicitly the configuration for *positive* bias voltage, so that the tip Fermi level is lower than the working electrode Fermi level. If all energies are counted from the Fermi energy of the working electrode, $\varepsilon_{Fsubstr}$, the empty redox level, ε_{ox}, is lowered with increasing negative η. The redox site is exposed to part of the bias voltage and also shifted relative to $\varepsilon_{Fsubstr}$ on *bias voltage* variation. Conformational and solvent polarization *fluctuations* as in electrochemical ET are, finally, crucial.

3.2. New interfacial (bio)electrochemical ET phenomena

The in situ STM results are most transparent when the bias voltage is small, i.e. [10,14,18]:

$$\gamma|eV_{bias}| < E_R - e\eta \tag{4}$$

γ is the fraction of the bias voltage at the site of the redox centre. The bias voltage is a "probing energy tip", and the "spectral resolution" better, the narrower the "probing tip". As the overpotential is raised, at fixed bias voltage, the cathodic current first rises due to more favourable driving force, but then drops as all active species are converted to reduced form, Fig. 2.

The following attractive form, with recognized limitations [19] applies for two-step ET via the molecular redox level [10,14,18]:

$$i_{tunn}^{symm} = \frac{1}{2} e n_{o/r} \frac{\omega_{eff}}{2\pi} \times \exp\left(-\frac{E_R - eV_{bias}}{4k_BT}\right)\left\{\cosh\left[\frac{(\frac{1}{2}-\gamma)eV_{bias} - \xi e\eta}{2k_BT}\right]\right\}^{-1} \tag{5}$$

Eq. (5) represents a process where the (bio)molecular redox centre is first reduced (oxidized) followed by re-oxidation (-reduction). The first single-ET event can, further be followed by a large number (exceeding a hundred or so) of subsequent events, represented by the quantity $n_{o/r}$, whilst the redox level relaxes through the energy window between the two Fermi levels. $n_{o/r}$ is large when the molecule-electrode electronic interactions are strong [14,19]. This is a novel ET *phenomenon* associated with in situ STM and holds a clue to the frequent observation of large tunnelling current densities, or conductivities (per molecule). Eq. (5) discloses a maximum at

$$\eta = \eta_{max} = \frac{1}{\xi}\left(\frac{1}{2} - \gamma\right)V_{bias} \tag{6}$$

If the redox centre in the gap is exposed to half the bias voltage drop, then $\gamma = \frac{1}{2}$, and the maximum is at $\eta_{max} = 0$, i.e. at the equilibrium redox potential, Sections 4 and 5. The precise location of the maximum depends, however, sensitively on the potential distribution in the tunnelling gap, as reflected by the parameters ξ and γ, Eqs. (5) and (6).

4. In situ imaging of bio-related redox molecules and linker molecules for PMV

4.1. Single-molecule imaging and interfacial ET of bio-related small redox molecules

Tao reported the first case of in situ STM spectroscopy using Fe-protoporphyrin IX on highly oriented pyrolytic graphite [25]. Single-molecule in situ STM of redox molecules is now an expanding area of single-molecule science. Fig. 3 shows examples of redox molecules imaged to single-molecule resolution and displaying two-step electrochemical tunnelling ET spectroscopy, Eqs. (5) and (6), specifically: (a) Organic redox molecules (viologen and tetrathiafulvalene [26]); (b) transition metal complexes (metalloporphyrins, polypyridine complexes of osmium and cobalt [27,28]); (c) and, an in situ prepared terpy-based Ru(II)/(III) complex [29].

In situ STS, Fig. 3 follows a sequential two-step ET pattern. The observations include [14]: (a) Single-molecule in situ STS resonance ("molecular transistor" or "diode" function); (b) systematic variation of the peak potential with the bias voltage; (c) in situ STS involving different metals with widely different electrochemical ET rate constants; (d) stochastic features with single-,

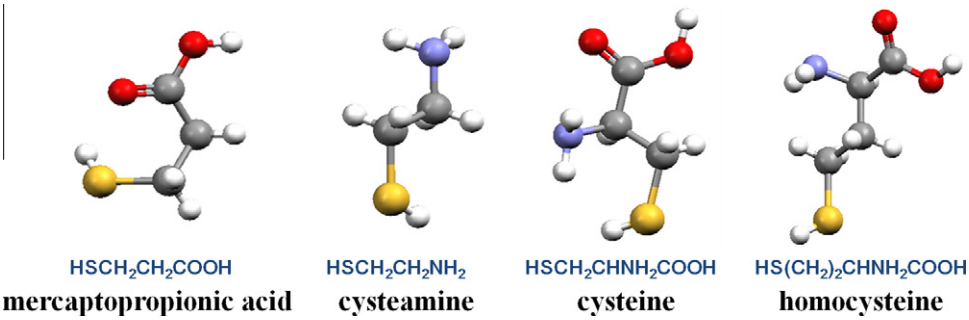

Fig. 4. Overview of some functionalized alkanethiol molecules imaged by in situ STM [30].

double-, triple- etc. molecular conductivity; and (e) coherent multi-ET in a single in situ STS event.

4.2. Functionalized alkanethiols

The two classes of biological chemical building blocks, amino acids and nucleobases have been prominent targets in single-molecule imaging of biological molecules. Functionalized alkanethiols and cysteine (Cys) have been particularly important also as linker groups in PMV.

4.2.1. Functionalized alkanethiols as linkers in PMV

The class of straight or branched, pure or functionalized alkanethiols are core molecular targets in single-molecule in situ STM, Fig. 4. Imaging has been closely tied to electrochemical ET of ordered alkanethiol-based SAMs where the reductive desorption process

$$Au - S - R + e^- \rightarrow Au + {}^-S - R \quad (12)$$

is crucial [14,30]. Alkanethiol-based SAMs have also been subject to large scale electronic structure computations disentangling STM in minute detail in both vacuum and aqueous environment.

Electrochemically controlled SAMs of the alkanethiol class characterized to molecular and sub-molecular in situ STM resolution has been reviewed recently [30]. We note here some issues of importance to functionalized alkanethiols as linker molecules for gentle immobilization of fully functional redox metalloprotein and metalloenzyme monolayers on single-crystal Au(111)-electrode surfaces. With a few exceptions, PMV is unstable or absent unless the electrode is modified by linker molecular SAMs, or the protein modified by non-native thiol-based amino acid residues. The thiol-based linker molecules adsorb strongly on the Au-surface. The opposite end holds a functional group that interacts "gently" with the protein, ascertaining that the latter retains full functional integrity. The interactions are often subtle. Closely related linker molecules can induce widely different voltammetric responses, and linker groups with no immediate expectable protein compatibility can arouse strong voltammetric signals.

The use of single-crystal electrodes enables surface structural characterization at the atomic and molecular level for pure and modified electrodes, directly in aqueous solution. Fig. 5 shows in situ STM of Au(111)- and Au(110)-electrode surfaces modified by thiol-based linker molecules, all of which form highly ordered monolayers, controlled by electrostatic and hydrogen bond networks [16,32]. The adsorption process can also be followed in real time through several intermediate phases [17,33]. The in situ STM images shown in Fig. 5 thus offer an unprecedentedly detailed view of the microenvironments for immobilized redox proteins "in voltammetric action".

4.2.2. Theoretical computations and STM image simulations

Multifarious patterns of widely different functionalized alkanethiol SAMs have been mapped to single-molecule resolution by in situ STM in aqueous electrolyte solution, strongly supported by electrochemical studies. In situ STM is, however, rooted in electronic *conductivity* and the quantum mechanical tunnelling effect. Theoretical support is therefore essential in detailed image interpretation of the many facets of alkanethiol-based SAM packing and in situ STM contrasts. We refer to recent studies of this important aspect [14,15,32,34,35].

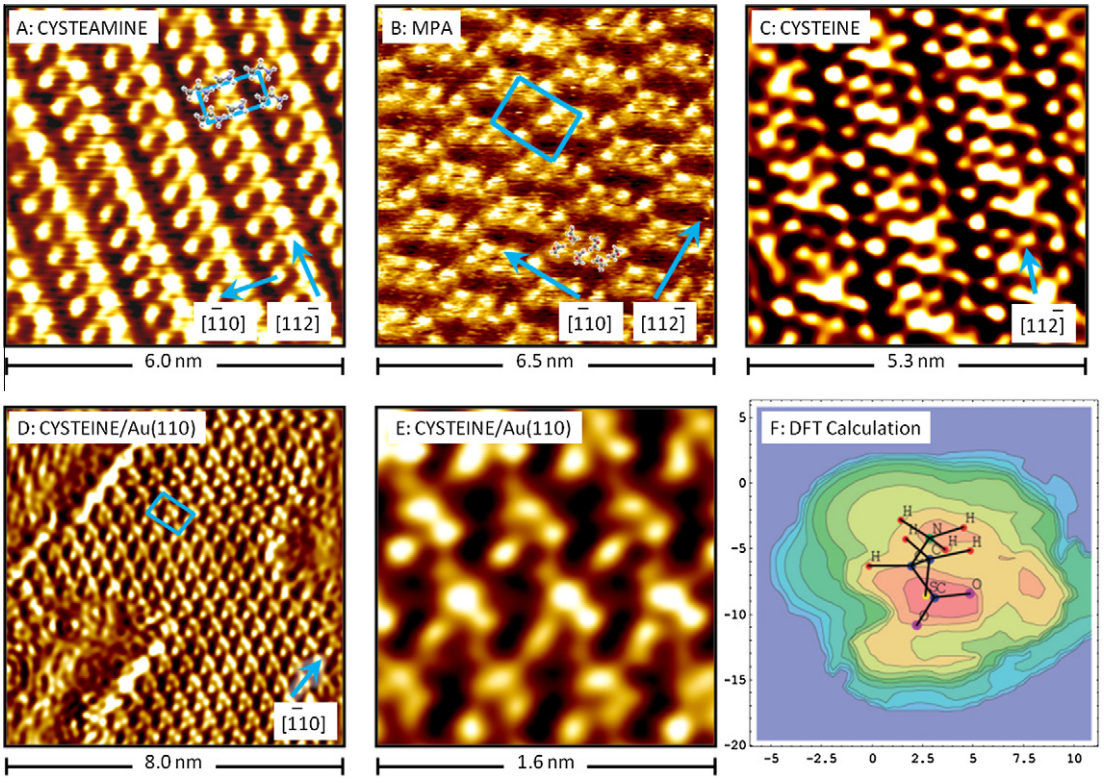

Fig. 5. High-resolution in situ STM of some alkanethiol-based molecules which are also linker molecules in PMV. Top row Au(111)-electrode surfaces; from left to right: Cysteamine [17], mercaptopropionic acid [31] and cysteine [15,16]. Bottom row Au(110)-electrode surfaces, from left to right: Cysteine surface lattice, zoom-in on the lattice to show the submolecular resolution, and DFT computed in situ STM image [15]. The latter shows that although the three in situ STM lobes originate from the three functional groups in the Cys molecule, they reflect the electronic densities (molecular orbitals) rather than the position of the O-, N-, and S-atoms.

5. Electrochemistry and in situ STM of single redox metalloprotein molecules

5.1. Metalloprotein voltammetry at bare and modified electrodes

Protein film voltammetry (PFV), reviewed extensively elsewhere, is established as a powerful tool in protein science, including mapping of molecular mechanisms of intramolecular and interfacial ET processes in surface bound protein systems [36–38]. PMV extends PFV to single-crystal electrode surfaces using linear, cyclic, fast-scan, square wave and differential pulse voltammetry, electrochemical impedance, X-ray photo-electron spectroscopy, the use of ultra-microelectrodes as well as gold nanoparticles, and microcantilever sensor technology [14]. Novel detail is emerging by single-molecule imaging. We address here some examples where metalloprotein mapping and functional control have reached the single-molecule level.

5.2. Single-molecule imaging of functional ET metalloproteins by in situ STM

Imaging of single protein molecules by STM and AFM in ambient air environment was reported early [39]. Electrochemically controlled in situ STM of proteins in natural aqueous biological media is much more recent. Figs. 6 and 7 show some redox metalloproteins on surfaces such as those shown in Fig. 5 imaged to single-molecule resolution by in situ STM. The molecules include the three ET metalloprotein classes, the blue copper – azurin in particular – heme group, and iron-sulfur proteins, Fig. 6. Other studies have addressed multi-centre redox metallo*enzymes* such as copper nitrite reductase, Fig. 7 [40] and de novo designed 4-α-helix proteins [41]. These studies illuminate both the powerful potential and some limitations of in situ STM.

A recent study of *Escherichia coli* wild-type and mutant 4α-helix cyt b_{562} [44] offered a successful approach addressing the heme

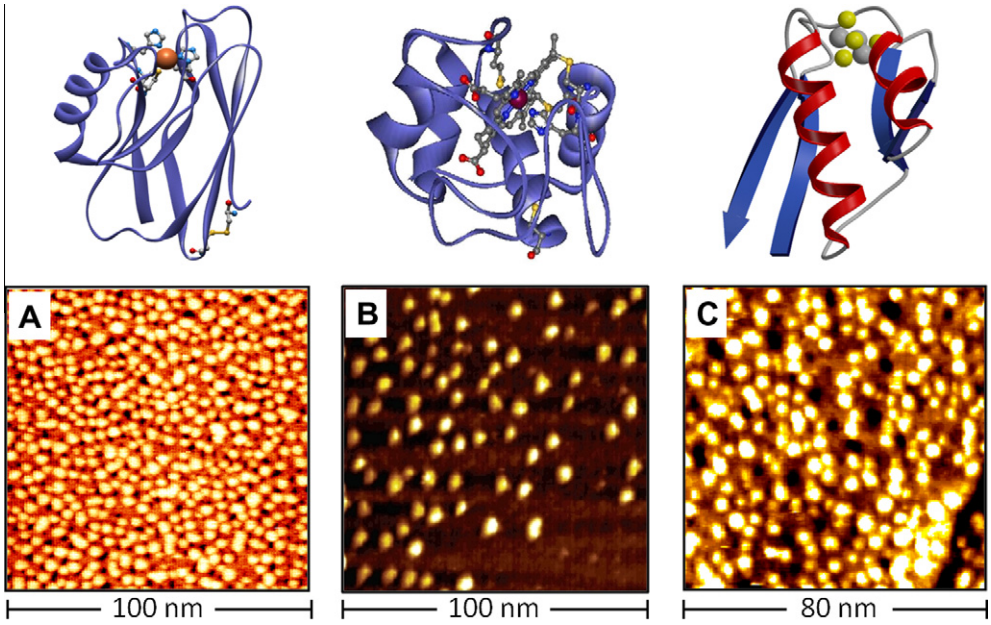

Fig. 6. Overview of three-dimensional structures (top row) and single-molecule in situ STM images (pure and SAM-modified Au(111)-electrode surfaces) of representatives of the three ET metalloprotein classes. Left: The blue copper protein *P. aeruginosa* azurin (PDB 4AZU) [42]; middle *S. cerevisiae* yeast cytochrome *c* (PDB 1YCC) [43]; right: *P. furiosus* ferredoxin [31].

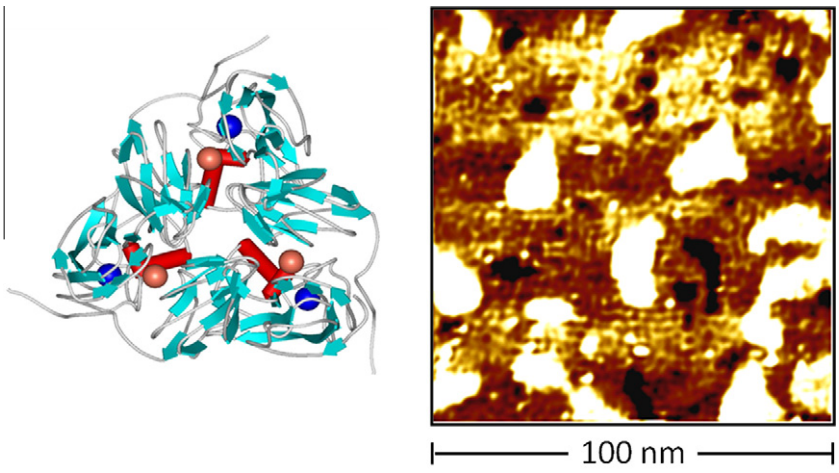

Fig. 7. Three-dimensional structure (left) and in situ STM image of *A. xylosoxidans* copper nitrite reductase (PDB 1HAU) directly in electrocatalytic action [40].

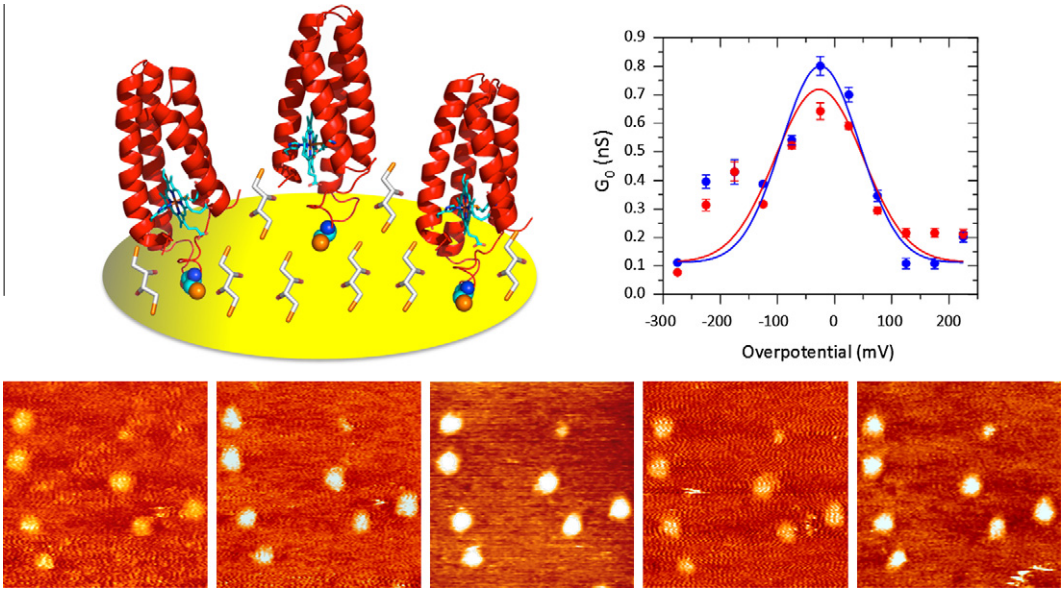

Fig. 8. The new single-molecule in situ STM target D50C Cyt b_{562} [44]. Top left: D50C cyt b_{562} on a Au(111)-electrode surface diluted in a 1,4-dithiothreitol co-adsorbed matrix (schematic). Top right: In situ tunnelling current/overpotential STS. Bottom row: Apparent D50C cyt b_{562} height dependence of the substrate electrode overpotential, following the pattern in the figure top, right.

protein class cyt b_{562} as a new class of single-molecule in situ STM and STS redox metalloprotein targets, Fig. 8. Cyt b_{562} is a bacterial periplasmic respiratory ET protein with a single heme group attached parallel to the α-helices by axial Met7 and His102 coordination. The D50C mutant protein, Fig. 8 has proved highly suitable for linking to Au(111)-electrode surfaces in sub-monolayers diluted in a 1,4-dithiothreitol (DTT) co-adsorbed matrix. Robust voltammetry (in contrast to the wild-type protein) and stable single-molecule in situ STM and STS were observed. The apparent height variation of adsorbed molecules with the electrochemical overpotential at constant bias voltage was recast as single-molecule normalized in situ STS. A strong spectroscopic feature around the equilibrium redox potential appeared as also observed previously for azurin [45] and for a range of small molecules [14], Section 4, Eq. (5).

5.3. Cytochrome c_4 – a prototype for microscopic electronic mapping of multi-centre redox metalloproteins

Biological ET is commonly controlled by large metalloproteins with several transition metal centres. Photosynthetic reaction centres, cyt *c* oxidase, and other redox enzyme complexes are examples. Intramolecular ET between the metal centres is a key function but "cooperativity" among the centres is another notion that implies that ET in a given centre affects the *microscopic* redox potentials and ET rate constants of all the other centres in overall "cooperative" charge transport. Cooperative mapping of the small four-heme redox metalloprotein cyt c_3 constituted life-long efforts of Antonio V. Xavier [46]. The number of electronic interactions is mostly prohibitive for microscopic mapping but *two-centre* metalloproteins represent prototype multi-centre redox metalloproteins with a simple enough electronic communication network that complete microscopic thermodynamic and kinetic ET mapping is within reach. The bacterial two-heme protein *Pseudomonas stutzeri* cyt c_4 has been investigated comprehensively in these contexts [47,48]. *P. stutzeri* cyt c_4 is organized in two domains, each with a single heme group, Fig. 9. The protein is strongly dipolar, with excess positive and negative charge (pH 7) on the C- and N-terminal domain, respectively. The redox potential difference is about 100 mV, with the higher potential associated with the C-terminal. This is crucial for electrostatic protein immobilization in specific orientations on SAM-modified Au(111)-electrodes. Spectroscopic and (un)folding data are also available. The heme groups are hydrogen bonded via two propionates but the 19 Å Fe–Fe *equilibrium* distance is not a likely configuration for intramolecular ET. Bimolecular ET with inorganic reaction partners disclosed no evidence of intramolecular ET up to 10–100 s^{-1} [48]. In contrast, the notably asymmetric CVs, Fig. 9 are only compatible with fast intramolecular ET (10–100 μs) in the electrochemical two-ET process [47]. Cyt c_4 is here oriented with the high-potential C-terminal domain adjacent to the negatively charged SAM-modified Au(111)-surface. This domain is reduced first in a cathodic scan followed by reduction of the remote N-terminal domain at the lower potential of this group, via intramolecular ET through the adjacent C-terminal domain. Re-oxidation of the low-potential heme, however, only begins when the higher potential of the adjacent heme is reached, again via fast intramolecular ET. *Gated* intramolecular ET triggered by protein binding to the electrode surface thus appears as a *P. stutzeri* cyt c_4 feature.

The strikingly different intramolecular ET rates of free and surface bound *P. stutzeri* cyt c_4 suggests that surface binding triggers intramolecular ET. Recent DFT computations show that the electronic overlap between the heme groups is exceedingly sensitive to the heme group orientation and increases by many orders of magnitude on hydrogen bond breaking and heme group relocation [49]. These views are supported by in situ STM, Fig. 9. The molecular structures observed correspond in size closely to a single cyt c_4 domain. In situ STM has therefore provided single-molecule structural and mechanistic support for the electrochemical ET behaviour of this protein.

6. Composite metalloproteins: blue Cu-oxidases and metalloprotein/nanoparticle hybrids

6.1. Single-molecule redox metalloenzymes in electrocatalytic action

In situ STM imaging and electrochemical control of redox metalloenzymes directly in enzyme action offers fascinating single-molecule perspectives. Such target molecules pose greater

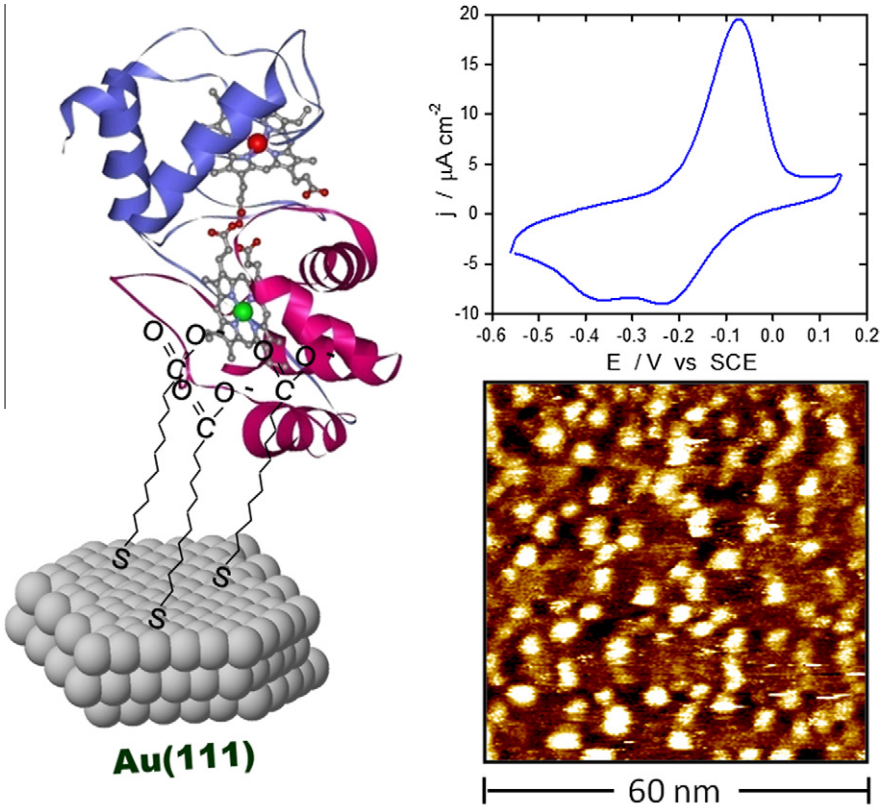

Fig. 9. Left: *P. stutzeri* cyt c_4 (PDB 1EPT) on a Au(111)-electrode surface modified by a mercaptodecanoic acid SAM. The positively charged high-potential C-terminal domain marked in red, the negatively charged N-terminal domain in blue. Top right: Cyclic voltammogram of *P. stutzeri* cyt c_4. The asymmetric appearance reflects the orientation of the molecule and intramolecular ET between the two heme groups as a core feature. Bottom right: In situ STM of *P. stutzeri* cyt c_4 on the mercaptodecanoic acid SAM modified Au(111)-electrode surface. The bright spots are individual *P. stutzeri* cyt c_4 molecules. The "spot" size corresponds to that of a single domain and supports the view of the protein in an upright orientation [47].

challenges than the smaller ET proteins. Recent – so far very few – studies illuminate these perspectives. The nitrite reductases (NiRs) are central in the biological nitrogen cycle where they catalyze the reduction of nitrite to lower oxidation states [50,51]. Rationales for the trimeric CuNiRs (each monomer molecular mass ≈ 36 kDa, here represented by *Achromobacter Xylosoxidans* CuNiR) as single-molecule in situ STM targets are, first that each monomer contains a type I blue copper centre for electron inlet, here from the working electrode, and a type II centre for catalytic NO_2^- -reduction. The two centres are directly linked, offering facile intramolecular ET, cf. cyt c_4. The enzyme substrate nitrite is, secondly a small molecule not detectable by in situ STM on the enzyme background. As frequently observed in enzyme voltammetry, binding of substrate induces, however, significant electronic changes in the enzyme [40,52,53], notably in the contact between the electron acceptor centre and the electrode surface. This resembles again cyt c_4 and offers prospects for electronic mapping of the enzyme in action at the single-molecule level.

A. xylosoxidans CuNiR is electrocatalytically active on SAM-modified Au(111)-electrode surfaces [40,53]. The voltammetric patterns are controlled by subtle hydrophilic and hydrophobic surface combinations of many surface linker molecules tested. A notable outcome is that the enzyme "in action" on cysteamine- and benzylthiol-modified Au(111)-electrode surfaces can be imaged in action at the single-molecule level, Fig. 7 [40,54]. Enzyme molecules even with the triangular crystallographic CuNiR structure are observed, and the molecular-scale contrasts *only* appear when nitrite is present. A recent study has disclosed a similar pattern for fungal laccase (*Streptomyces coelicolor*) for which substrate dioxygen also triggers intramolecular ET and strong in situ STM contrasts [55]. In situ STM of CuNiR and the laccases has thus opened the area of single-molecule electrochemical redox metalloenzyme activity. These novel observations can be compared with more established single-molecule fluorescence-based enzyme kinetics [14,56].

6.2. Electrochemistry of Au-nanoparticle/metalloprotein hybrids

Inorganic particles and other structures have reached the size range of biomolecules such as proteins. This is also the range where electronic properties transform from macroscopic to single-molecule behaviour. The *combination* of inorganic metallic or semiconductor structures with comparable-size (bio)molecules into "hybrid" structures has become a new core notion [57–59].

Solute monolayer-coated ("capped") AuNPs are central in colloid and surface science. Facile chemical synthesis introduced by Schmid [60] and by Brust and Schiffrin [61] have strongly boosted AuNP and other metal-NP science. The smallest, i.e. ⩽1 nm particles behave like a similar-size molecule with a discrete electronic spectrum or a wide HOMO/LUMO gap [62–64]. Intermediate-size AuNPs, say 1.6 nm (Au_{145}) to 2.5 nm (many hundred Au-atoms) display Coulomb charging effects [64] while the Coulomb energy spacings in larger AuNPs (⩾ 3–5 nm) are too close for discreteness-of-charge effects. Protected AuNPs combined with redox metalloproteins into "hybrids", are important in bioelectrocatalysis, with links to biological diagnostics [58]. A recent study of a "hybrid" between a 3 nm AuNP and *P. aeruginosa* azurin illuminates interfacial electrochemical ET and in situ STM of a protein/NP hybrid [57].

P. aeruginosa azurin can be linked by strong hydrophobic forces to alkanethiol-protected 3 nm AuNPs in turn immobilized on a Au(111)-electrode surface via an aromatic 4,4′-biphenyl-dithiol linker. Notably, the AuNP hydrophobically linked to azurin increases the ET rate by at least an order of magnitude compared to azurin alone on similar alkanethiol-modified surfaces, in spite of a 4 nm ET distance increase. A two-step, azurin/AuNP and AuNP/electrode ET mechanism accords with the data. The dual voltammetric pattern also accords with dual in situ STM contrasts with a weaker, fluctuating contrast assigned to the AuNP/azurin hybrid and a stronger robust contrast to displaced AuNPs or azurin molecules.

7. Concluding observations and some perspectives

Single-crystal, atomically planar electrode surfaces have paved the way for in situ STM and AFM in bioelectrochemistry. In situ STM has increased structural resolution of metalloproteins and small biomolecules on (bio)electrochemical electrode surfaces to the molecular and sometimes sub-molecular levels. Dynamic phenomena such as phase transitions and the monolayer formation *process* can also be followed. The image detail in both individual adsorbate molecules and their lateral organization offers understanding of the interaction of "biological liquids" with solid surfaces. As in situ STM is based on molecular electronic conductivity, we have also included a short theoretical discussion of single-molecule interfacial ET processes, with focus on "natural" biomolecular aqueous solution environment, and electrochemically controlled (bio)molecular function. Single-molecule resolution of the molecules (particularly proteins) fully active in ET or enzyme function is achieved. Not only structural mapping but also ET, redox enzyme *function*, and cooperative phenomena can be addressed, illuminated by azurin, cyt b_{562}, cyt c_4, and CuNiR. Biomolecular "electronics", enzyme electrochemistry, and biological single-molecule screening are attractive applied perspectives of the new bioelectrochemistry. *Fundamental* bioelectrochemical innovation including theoretical support remains, however, crucial pre-requisites.

Acknowledgement

This work is supported by the Danish Research Council for Technology and Production, the Lundbeck Foundation, and the Villum Kann Rasmussen Foundation.

References

[1] Lustenberger, P., Rohrer, H., Christoph, R. and Siegenthaler, H. (1988) Scanning tunneling microscopy at potential controlled electrode surfaces in electrolytic environment. J. Electroanal. Chem. 243, 225–235.
[2] Wiechers, J., Twomey, T., Kolb, D.M. and Behm, R.J. (1988) An in situ scanning tunneling microscopy study of Au(111) with atomic scale resolution. J. Electroanal. Chem. 248, 451–460.
[3] Gewirth, A.A. and Niece, B.K. (1997) Electrochemical applications of in situ scanning probe microscopy. Chem. Rev. 97, 1129–1162.
[4] Wieckowski, A., Ed., (1999). Interfacial Electrochemistry. Theory, Experiment and Applications, Marcel Dekker, New York.
[5] Carnie, S.L. and Torrie, G.M. (1984) The statistical-mechanics of the electrical double-layer. Adv. Chem. Phys. 56, 141–253.
[6] Kornyshev, A.A. (1988) Solvation of a metal surface in: The Chemical Physics of Solvation. Part C. Solvation Phenomena in Specific Physical Chemical and Biological Systems (Dogonadze, R.R., Kálmán, E., Kornyshev, A.A. and Ulstrup, J., Eds.), pp. 355–400, Elsevier, Amsterdam.
[7] Kolb, D.M. (2001) Electrochemical surface science. Ang. Chem.-Int. Ed. 40, 1162–1181.
[8] Kuznetsov, A.M. (1995) Charge Transfer in Physics, Chemistry and Biology, Gordon & Breach, Reading.
[9] Kuznetsov, A.M. and Ulstrup, J. (1999) Electron Transfer in Chemistry and Biology: An Introduction to the Theory, Wiley, Chichester.
[10] Kuznetsov, A.M. and Ulstrup, J. (2000) Mechanisms of in situ scanning tunnelling microscopy of organized redox molecular assemblies. J. Phys. Chem. A 104, 11531–11540.
[11] Marcus, R.A. (1956) On the theory of oxidation-reduction reactions involving electron transfer 1. J. Chem. Phys. 24, 966–978.
[12] Iversen, G., Kharkats, Y.I. and Ulstrup, J. (1998) Simple dielectric image charge models for electrostatic interactions in metalloproteins. Mol. Phys. 94, 297–306.
[13] Kuznetsov, A.M. and Ulstrup, J. (1982) On the Theory of Long-Range Electron Hopping in Polar Media. Phys. Status Solidi B: Basic Res. 114, 673–683.
[14] Zhang, J.D., Kuznetsov, A.M., Medvedev, I.G., Chi, Q.J., Albrecht, T., Jensen, P.S. and Ulstrup, J. (2008) Single-molecule electron transfer in electrochemical environments. Chem. Rev. 108, 2737–2791.
[15] Zhang, J.D., Chi, Q.J., Nazmutdinov, R.R., Zinkicheva, T.T. and Bronshtein, M.D. (2009) Submolecular electronic mapping of single cysteine molecules by in situ scanning tunneling imaging. Langmuir 25, 2232–2240.
[16] Zhang, J.D., Chi, Q.J., Nielsen, J.U., Friis, E.P., Andersen, J.E.T. and Ulstrup, J. (2000) Two-dimensional cysteine and cystine cluster networks on Au(111) disclosed by voltammetry and in situ scanning tunneling microscopy. Langmuir 16, 7229–7237.
[17] Zhang, J.D., Bilič, A., Reimers, J.R., Hush, N.S. and Ulstrup, J. (2005) Coexistence of multiple conformations in cysteamine monolayers on Au(111). J. Phys. Chem. B 109, 15355–15367.
[18] Kuznetsov, A.M. and Ulstrup, J. (2001) Mechanisms of in situ scanning tunnelling microscopy of organized redox molecular assemblies (vol. 104A, pp. 11531, 2000). J. Phys. Chem. A 105, 7494.
[19] Albrecht, T., Guckian, A., Kuznetsov, A.M., Vos, J.G. and Ulstrup, J. (2006) Mechanism of electrochemical charge transport in individual transition metal complexes. J. Am. Chem. Soc. 128, 17132–17138.
[20] Kuznetsov, A.M., Vigdorovich, M.D. and Ulstrup, J. (1993) Self-consistent environmental fluctuation effects on the electronic tunnel factor and the activation Gibbs energy in long-range electron-transfer. Chem. Phys. 176, 539–554.
[21] Kuznetsov, A.M. and Ulstrup, J. (1999) Simple schemes in chemical electron transfer formalism beyond single-mode quadratic forms: environmental vibrational dispersion and anharmonic nuclear motion. Phys. Chem. Chem. Phys. 1, 5587–5592.
[22] Saveant, J.M. (1987) A simple-model for the kinetics of dissociative electron-transfer in polar-solvents – application to the homogeneous and heterogeneous reduction of alkyl-halides. J. Am. Chem. Soc. 109, 6788–6795.
[23] German, E.D. and Kuznetsov, A.M. (1994) Quantum-mechanical theory of dissociative electron-transfer in polar-solvents. J. Phys. Chem. 98, 6120–6127.
[24] Louro, R., Catarino, T., Paquete, C. and Turner, D. (2004) Distance dependence of interactions between charged centres in proteins with common structural features RID B-8267-2009. FEBS Lett. 576, 77–80.
[25] Tao, N.J. (1996) Probing potential-tuned resonant tunneling through redox molecules with scanning tunneling microscopy. Phys. Rev. Lett. 76, 4066–4069.
[26] Leary, E., Higgins, S.J., van Zalinge, H., Haiss, W., Nichols, R.J., Nygaard, S., Jeppesen, J.O. and Ulstrup, J. (2008) Structure-property relationships in redox-gated single molecule junctions – A comparison of pyrrolo-tetrathiafulvalene and viologen redox groups. J. Am. Chem. Soc. 130, 12204–12205.
[27] Albrecht, T., Moth-Poulsen, K., Christensen, J.B., Guckian, A., Bjornholm, T., Vos, J.G. and Ulstrup, J. (2006) In situ scanning tunnelling spectroscopy of inorganic transition metal complexes. Faraday Discuss. 131, 265–279.
[28] Yoshimoto, S., Tsutsumi, E., Suto, K., Honda, Y. and Itaya, K. (2005) Molecular assemblies and redox reactions of zinc(II) tetraphenylporphyrin and zinc(II) phthalocyanine on Au(111) single crystal surface at electrochemical interface. Chem. Phys. 319, 147–158. and references therein.
[29] Salvatore, P., Hansen, A.G., Moth-Poulsen, K., Bjørnholm, T., Nichols, R.J. and Ulstrup, J. (2011) Voltammetry and in situ scanning tunnelling spectroscopy of osmium, iron, and ruthenium complexes of 2,2′:6′,2″-terpyridine covalently linked to Au(111)-electrodes. Phys. Chem. Chem. Phys. 13, 14394–14403.
[30] Zhang, J., Welinder, A.C., Chi, Q. and Ulstrup, J. (2011) Electrochemically controlled self-assembled monolayers characterized with molecular and sub-molecular resolution. Phys. Chem. Chem. Phys. 13, 5526–5545.
[31] Zhang, J.D., Christensen, H.E.M., Ooi, B.L. and Ulstrup, J. (2004) In situ STM imaging and direct electrochemistry of Pyrococcus furiosus ferredoxin assembled on thiolate-modified Au(111) surfaces. Langmuir 20, 10200–10207.
[32] Nazmutdinov, R.R., Zhang, J.D., Zinkicheva, T.T., Manyurov, I.R. and Ulstrup, J. (2006) Adsorption and in situ scanning tunneling microscopy of cysteine on Au(111): structure, energy, and tunneling contrasts. Langmuir 22, 7556–7567.
[33] Zhang, J.D., Chi, Q.J. and Ulstrup, J. (2006) Assembly dynamics and detailed structure of 1-propanethiol monolayers on Au(111) surfaces observed real time by in situ STM. Langmuir 22, 6203–6213.
[34] Bilič, A., Reimers, J.R. and Hush, N.S. (2005) The structure, energetics, and nature of the chemical bonding of phenylthiol adsorbed on the Au(111) surface. Implications for density-functional calculations of molecular-electronic conduction. J. Chem. Phys. 122, 094708.
[35] Wang, Y., Chi, Q., Hush, N.S., Reimers, J.R., Zhang, J. and Ulstrup, J. (2011) Gold mining by alkanethiol radicals: vacancies and pits in the self-assembled monolayers of 1-propanethiol and 1-butanethiol on Au(111). J. Phys. Chem. C 115, 10630–10639.
[36] Armstrong, F.A. (2002) Insights from protein film voltammetry into mechanisms of complex biological electron-transfer reactions. J. Chem. Soc.-Dalton Trans., 661–671.

[37] Ferapontova, E. and Gorton, L. (2003) Bioelectrocatalytical detection of H_2O_2 with different forms of horseradish peroxidase directly adsorbed at polycrystalline silver and gold. Electroanalysis 15, 484–491.
[38] Leger, C. and Bertrand, P. (2008) Direct electrochemistry of redox enzymes as a tool for mechanistic studies. Chem. Rev. 108, 2379–2438.
[39] Zhang, J., Chi, Q., Kuznetsov, A.M., Hansen, A.G., Wackerbarth, H., Christensen, H.E.M., Andersen, J.E.T. and Ulstrup, J. (2002) Electronic properties of functional biomolecules at metal/aqueous solution interfaces. J. Phys. Chem. B 106, 1131–1152.
[40] Zhang, J.D., Welinder, A.C., Hansen, A.G., Christensen, H.E.M. and Ulstrup, J. (2003) Catalytic monolayer voltammetry and in situ scanning tunneling microscopy of copper nitrite reductase on cysteamine-modified Au(111) electrodes. J. Phys. Chem. B 107, 12480–12484.
[41] Albrecht, T., Li, W., Haehnel, W., Hildebrandt, P. and Ulstrup, J. (2006) Voltammetry and in situ scanning tunnelling microscopy of de novo designed heme protein monolayers on Au(111)-electrode surfaces. Bioelectrochemistry 69, 193–200.
[42] Chi, Q.J., Zhang, J.D., Nielsen, J.U., Friis, E.P., Chorkendorff, I., Canters, G.W., Andersen, J.E.T. and Ulstrup, J. (2000) Molecular monolayers and interfacial electron transfer of *Pseudomonas aeruginosa* azurin on Au(111). J. Am. Chem. Soc. 122, 4047–4055.
[43] Hansen, A.G., Boisen, A., Nielsen, J.U., Wackerbarth, H., Chorkendorff, I., Andersen, J.E.T., Zhang, J.D. and Ulstrup, J. (2003) Adsorption and interfacial electron transfer of *Saccharomyces cerevisiae* yeast cytochrome c monolayers on Au(111) electrodes. Langmuir 19, 3419–3427.
[44] Della Pia, E., Chi, Q., Jones, D.D., Macdonald, J.E., Ulstrup, J. and Elliott, M. (2011) Single-molecule mapping of long-range electron transport for a cytochrome b_{562} variant. Nano Lett. 11, 176–182.
[45] Chi, Q., Farver, O. and Ulstrup, J. (2005) Long-range protein electron transfer observed at the single-molecule level: In situ mapping of redox-gated tunneling resonance. Proc. Natl Acad. Sci. USA 102, 16203–16208.
[46] Paquete, C.M., Turner, D.L., Louro, R.O., Xavier, A.V. and Catarino, T. (2007) Thermodynamic and kinetic characterisation of individual haems in multicentre cytochromes c(3) RID B-8267–2009. Biochim. Biophys. Acta-Bioenerget. 1767, 1169–1179.
[47] Chi, Q.J., Zhang, J.D., Arslan, T., Borg, L., Pedersen, G.W., Christensen, H.E.M., Nazmudtinov, R.R. and Ulstrup, J. (2010) Approach to interfacial and intramolecular electron transfer of the diheme protein cytochrome c(4) assembled on Au(111) surfaces. J. Phys. Chem. B 114, 5617–5624.
[48] Raffalt, A.C., Schmidt, L., Christensen, H.E.M., Chi, Q. and Ulstrup, J. (2009) Electron transfer patterns of the di-heme protein cytochrome c(4) from *Pseudomonas stutzeri*. J. Inorg. Biochem. 103, 717–722.
[49] Nazmudtinov, R.R., Bronshtein, M.D., Zinkicheva, T.T., Chi, Q., Zhang, J., Ulstrup, J. (submitted for publication) Intramolecular electron transfer in the di-heme protein *Pseudonas stutzeri* cytochrome c_4: Model prediction of kinetic parameters.
[50] Richardson, D.J. and Watmough, N.J. (1999) Inorganic nitrogen metabolism in bacteria. Curr. Opin. Chem. Biol. 3, 207–219.
[51] Simon, J. (2002) Enzymology and bioenergetics of respiratory nitrite ammonification. FEMS Microbiol. Rev. 26, 285–309.
[52] Armstrong, F.A. (2005) Recent developments in dynamic electrochemical studies of adsorbed enzymes and their active sites. Curr. Opin. Chem. Biol. 9, 110–117.
[53] Welinder, A.C., Zhang, J., Hansen, A.G., Moth-Poulsen, K., Christensen, H.E.M., Kuznetsov, A.M., Bjornholm, T. and Ulstrup, J. (2007) Voltammetry and electrocatalysis of achrornobacter xylosoxidans copper nitrite reductase on functionalized Au(111)-electrode surfaces. Z. Phys. Chem.-Int. J. Res. Phys. Chem. Chem. Phys. 221, 1343–1378.
[54] Chi, Q.J., Zhang, J.D., Jensen, P.S., Christensen, H.E.M. and Ulstrup, J. (2006) Long-range interfacial electron transfer of metalloproteins based on molecular wiring assemblies. Faraday Discuss. 131, 181–195.
[55] Climent, V., Zhang, J., Friis, E.P., Østergaard, L.H., Ulstrup, J. Bioelectrocatalysis and in situ scanning tunneling microscopy of dioxygen reduction by Laccases and Bilrubin oxidase on single-crystal Au(111)-electrode surfaces, submitted for publication.
[56] Min, W., English, B.P., Luo, G.B., Cherayil, B.J., Kou, S.C. and Xie, X.S. (2005) Fluctuating enzymes: Lessons from single-molecule studies. Acc. Chem. Res. 38, 923–931.
[57] Jensen, P.S., Chi, Q., Zhang, J. and Ulstrup, J. (2009) Long-range interfacial electrochemical electron transfer of *Pseudomonas aeruginosa* azurin-gold nanoparticle hybrid systems. J. Phys. Chem. C 113, 13993–14000.
[58] Katz, E. and Willner, I. (2004) Integrated nanoparticle-biomolecule hybrid systems: synthesis, properties, and applications. Ang. Chem.-Int. Ed. 43, 6042–6108.
[59] Jensen, P.S., Chi, Q., Grumsen, F.B., Abad, J.M., Horsewell, A., Schiffrin, D.J. and Ulstrup, J. (2007) Gold nanoparticle assisted assembly of a heme protein for enhancement of long-range interfacial electron transfer. J. Phys. Chem. C 111, 6124–6132.
[60] Schmid, G., Pfeil, R., Boese, R., Bandermann, F., Meyer, S., Calis, G.H.M. and Vandervelden, W.A. (1981) $Au_{55}[P(C_6H_5)_3]_{12}Cl_6$ – a gold cluster of an exceptional size. Chem. Ber. Recl. 114, 3634–3642.
[61] Brust, M., Walker, M., Bethell, D., Schiffrin, D.J. and Whyman, R. (1994) Synthesis of thiol-derivatized gold nanoparticles in a 2-phase liquid–liquid system. J. Chem. Soc.-Chem. Commun., 801–802.
[62] Quinn, B.M., Liljeroth, P., Ruiz, V., Laaksonen, T. and Kontturi, K. (2003) Electrochemical resolution of 15 oxidation states for monolayer protected gold nanoparticles. J. Am. Chem. Soc. 125, 6644–6645.
[63] Chen, S.W., Murray, R.W. and Feldberg, S.W. (1998) Quantized capacitance charging of monolayer-protected Au clusters. J. Phys. Chem. B 102, 9898–9907.
[64] Albrecht, T., Mertens, S.F.L. and Ulstrup, J. (2007) Intrinsic multistate switching of gold clusters through electrochemical gating. J. Am. Chem. Soc. 129, 9162–9167.